Surface Science 606 (2012) 1918–1921

Contents lists available at SciVerse ScienceDirect

Surface Science

journal homepage: www.elsevier.com/locate/susc

Structural analysis of Si(111)-√21×√21-(Ag, Cs) surface by reflection high-energy positron diffraction

Y. Fukaya [a,*], I. Matsuda [b], R. Yukawa [b], A. Kawasuso [a]

[a] Advanced Science Research Center, Japan Atomic Energy Agency, 1233 Watanuki, Takasaki, Gunma 370-1292, Japan
[b] ISSP, University of Tokyo, 5-1-5, Kashiwanoha, Kashiwa, Chiba 277-8581, Japan

ARTICLE INFO

Article history:
Received 23 December 2011
Accepted 31 July 2012
Available online 4 August 2012

Keywords:
Surface structure
Silicon
Silver
Cesium
Reflection high-energy positron diffraction (RHEPD)

ABSTRACT

We have investigated the Si(111)-√21×√21-(Ag, Cs) superstructure using reflection high-energy positron diffraction. Rocking curve analysis based on the dynamical diffraction theory reveals that Cs atoms are located at a height of 3.04 Å above the underlying √3×√3-Ag structure and that they form a triangular structure with a side length of 10.12 Å. The structure of the Si(111)-√21×√21-(Ag, Cs) surface is significantly different from those of the Si(111)-√21×√21-Ag and Si(111)-√21×√21-(Ag, Au) surfaces, probably because of the different electronic structures of the alkali and noble metal atoms.

1. Introduction

Extensive studies have been carried out on the surface of Si(111)-√3×√3-Ag, as a typical two-dimensional metal system [1,2]. Adsorption of small amounts of noble (Cu, Ag, and Au) or alkali (Na, K, and Cs) metal atoms on this surface results in the formation of √21×√21 superstructures with a sharp increase in the surface electrical conductivity [1,2]. From the metallurgical point of view, √21×√21 superstructures have attracted attention as two-dimensional electron compound alloys [3,4]. Recently, Matsuda et al. investigated the interaction energy among adatoms in the √21×√21 superstructures by considering them as electron compounds [5,6]. They demonstrated that the interaction among the adatoms can be explained in terms of the pseudopotential model [5].

The atomic coordinates of √21×√21 superstructures have been studied both experimentally [7–13] and theoretically [14–16]. In the cases of Si(111)-√21×√21-Ag and Si(111)-√21×√21-(Ag, Au), we found that three adatoms are situated at the centers of large Ag triangles surrounding the Si trimers in a unit cell [12,13]. Although the electronic states of alkali-metal-induced Si(111)-√21×√21 surfaces resemble those of noble-metal-induced Si(111)-√21×√21 surfaces [17], their structures are considered to be different, as seen in scanning tunneling microscopy (STM) observations [18]. In this study, we measured the rocking curves for the Si(111)-√21×√21-(Ag, Cs) surface by reflection high-energy positron diffraction (RHEPD) and determined the structure of the surface. We also discussed the difference between the noble- and alkali-metal-induced √21×√21 superstructures.

2. Experimental procedure

Substrates ($10\times5\times0.5$ mm^3) were cut from a mirror-polished *n*-type Si(111) wafer with a resistivity of 1–10 Ω cm. These substrates were transferred into an ultra-high vacuum (UHV) chamber with a base pressure less than 3×10^{-8} Pa. After degassing at 670 K for 3 h, by flashing at 1470 K for a few seconds, clean 7×7 structures were formed on these substrate surfaces. Subsequently, by depositing one monolayer (ML) of Ag atoms on the 7×7 structures at 740 K (1 ML = 7.83×10^{14} cm^{-2}), √3×√3-Ag structures were formed. Finally, after the deposition of 0.14 ± 0.01 ML of Cs atoms at 160 K, well-ordered Si(111)-√21×√21-(Ag, Cs) surfaces were formed. The deposition rate of Cs atoms was calibrated by the formations of 6×6-(Ag, Cs) and √21×√21-(Ag, Cs) surfaces [8].

RHEPD measurements were carried out using a highly parallel and focused positron beam generated from a ^{22}Na positron source and electromagnetic lenses. The positron beam energy was 10 keV. The diffraction patterns were observed using a microchannel plate with a phosphor screen and a charge-coupled-device camera. For rocking curve measurements, the glancing angle (θ) of the incident positron beam was changed from 0.3° to 6.0° in steps of 0.1° by rotating the sample. The details of experimental setup were described elsewhere [19].

* Corresponding author. Tel.: +81 27 346 9330; fax: +81 27 346 9432.
E-mail address: fukaya.yuki99@jaea.go.jp (Y. Fukaya).

0039-6028/$ – see front matter © 2012 Elsevier B.V. All rights reserved.
http://dx.doi.org/10.1016/j.susc.2012.07.039

3. Results and discussion

The open circles in Fig. 1 represent the RHEPD rocking curve of the Si(111)-$\sqrt{21}\times\sqrt{21}$-(Ag, Cs) surface at 140 K. The azimuth of the incident beam is 7.5° with respect to the [11$\bar{2}$] direction (the so-called one-beam condition [20]). Under this condition, the RHEPD intensity of a specular spot mainly depends on atomic positions perpendicular to the surface. In the total reflection region [21], two distinct dip structures appear, one at around 1.2° and the other at around 2.2°. These dip structures are quite different from those observed for the Si(111)-$\sqrt{21}\times\sqrt{21}$-Ag and Si(111)-$\sqrt{21}\times\sqrt{21}$-(Ag, Au) surfaces, which show strong total reflections and (111) Bragg reflections [12,13]. The above result indicates that the height of the Cs atoms is relatively higher than the underlying Ag layer.

To determine the height of the Cs atoms from the underlying Ag layer, we compare the experimental and calculated rocking curves on the basis of the dynamical diffraction theory [22]. For the calculations, we assume the thermal vibration amplitudes for the Ag and Cs, and Si atoms to be 1.09×10^{-1} and 5.62×10^{-2} Å, respectively [12,13]. The absorption potentials due to the electronic excitations (single-electron and plasmon) for the Ag and Cs and Si layers were taken to be 0 and 1.70 eV, respectively [12,13,23]. The underlying layers were assumed to have the inequivalent triangle (IET) structure. The black lines in Fig. 1 show the calculated RHEPD rocking curves for Cs atoms at different heights (h_{ad}) from the underlying Ag layer (also see Fig. 3(a)). A dip appears at $\theta=1.6°$ for $h_{ad}=2$ Å, two dips appear at $\theta=1.2°$ and 2.1° for $h_{ad}=3$ Å, and three dips appear at $\theta=0.8°$, 1.5°, and 2.2° for $h_{ad}=4$ Å. The appearance of multiple dips for increasing values of h_{ad} is due to the interference between the positron beams reflected from the adatom and the underlying Ag layers [24]. Fig. 1(b) shows the reliability factor (R) as a function of h_{ad}. There are two local minima of R at $h_{ad}=1.20$ and 3.04 Å. The value of 1.20 Å should be an artificial coincidence because the dip structures in the curves calculated using $h_{ad}=1.20$ Å do not reproduce those ($\theta=1.2°$ and 2.2°) in the measured curve, as shown in Fig. 1(a). In considering the dip structures and the minimum value of R, we obtained at $h_{ad}=3.04\pm0.26$ Å. As shown by the red line in Fig. 1(a), when $h_{ad}=3.04$ Å, the calculations best reproduced the experimental results. This height of the Cs atoms from the underlying Ag layer was much greater than those of the Ag and Au atoms on the Si(111)-$\sqrt{21}\times\sqrt{21}$-Ag and Si(111)-$\sqrt{21}\times\sqrt{21}$-(Ag, Au) surfaces (0.53–0.59 Å) [12,13].

Fig. 2(a) shows the RHEPD rocking curves of the (0 0), (1/3 1/3), and (2/3 2/3) spots from the Si(111)-$\sqrt{21}\times\sqrt{21}$-(Ag, Cs) surface in the [11$\bar{2}$] direction at 140 K. It should be noted that since the surface is composed of the double domains of the $\sqrt{21}\times\sqrt{21}(R\pm10.89°)$

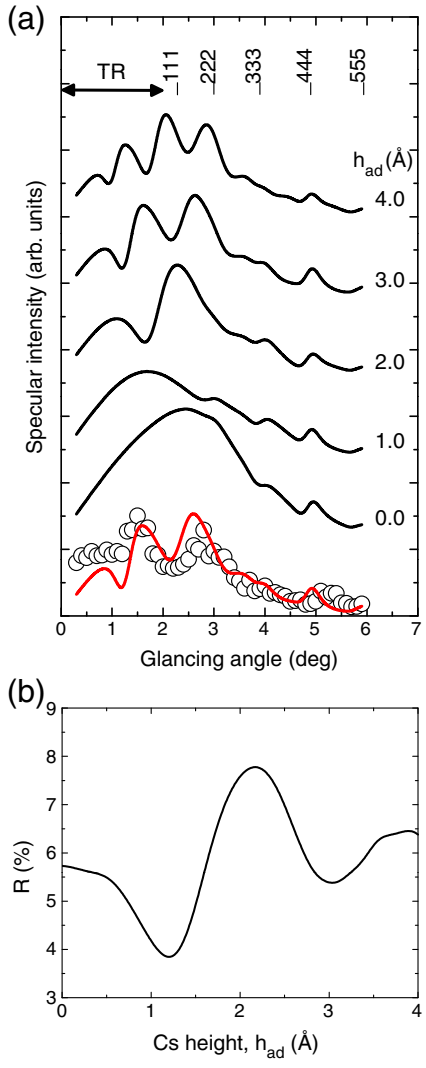

Fig. 1. (a) RHEPD rocking curves of the specular spot from the Si(111)-$\sqrt{21}\times\sqrt{21}$-(Ag, Cs) surface under the one-beam condition. The incident azimuth of the positron beam is 7.5° with respect to the [11$\bar{2}$] direction. The open circles denote the experimental curve at 140 K. The black solid lines indicate the calculated curves for various heights (h_{ad}) of the Cs atoms from the underlying Ag layer. The red solid line indicates the curve calculated using the optimum adatom height. TR stands for total reflection region. (b) Reliability factor (R) between the experimental and calculated rocking curves under the one-beam condition as a function of h_{ad}.

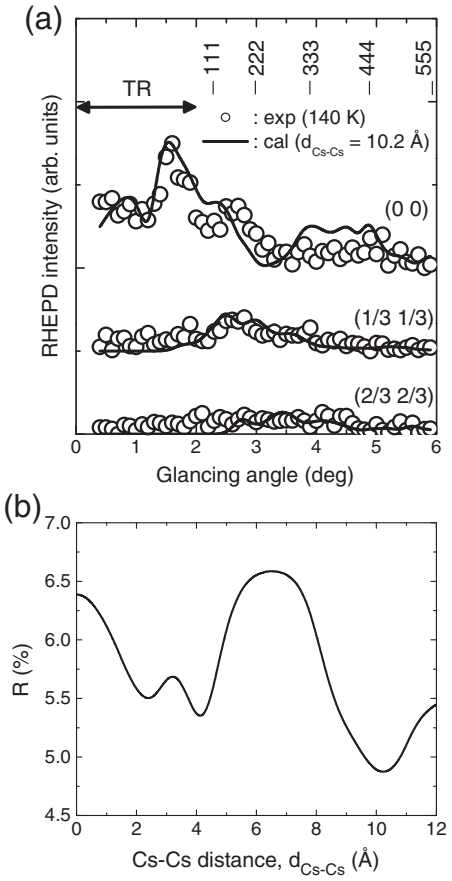

Fig. 2. (a) RHEPD rocking curves of the (00), (1/3 1/3), and (2/3 2/3) spots from the Si(111)-$\sqrt{21}\times\sqrt{21}$-(Ag, Cs) surface in the [11$\bar{2}$] direction at 140 K. The open circles and solid lines denote the experimental curves and the calculated curves determined using the optimum d_{Cs-Cs}, respectively. (b) Reliability factor (R) between the experimental and calculated rocking curves as a function of d_{Cs-Cs}.

structures [8], the (1/3 1/3) and (2/3 2/3) spots from the double domains are overlapped. To determine the in-plane adsorption sites of the Cs atoms, we calculated the RHEPD rocking curves in the [$11\bar{2}$] direction on the basis of the dynamical diffraction theory, taking into account the double domains. The STM observations [11] revealed that the Cs atoms arrange themselves in triangular structures on the underlying $\sqrt{3}\times\sqrt{3}$-Ag structure. Thus, in the calculations, the side length (d_{Cs-Cs}) and adsorption sites are assumed to be fitting parameters (also see Fig. 3(a)). Fig. 2(b) shows the reliability factor R determined for the rocking curves of the (0 0), (1/3 1/3), and (2/3 2/3) spots for various values of d_{Cs-Cs} when the center of the Cs triangle coincides with the center of the Si trimer. Minimum value of R is obtained at $d_{Cs-Cs}=10.12\pm1.72$ Å. It is interesting to note that two local minima appear at $d_{Cs-Cs}=2.2$ and 4.1 Å. In considering the ionic radius (1.67–1.88 Å) of Cs atoms and the repulsive force among the ions, $d_{Cs-Cs}=2.2$ and 4.1 Å are physically unacceptable. Even though the rocking curve is reproduced, it should be an artificial coincidence. The variation of R as a function of d_{Cs-Cs} was nearly the same (within $\pm$0.2%) for different positions of the Cs triangles.

Thus, the optimum value of d_{Cs-Cs} is determined to be 10.12 Å. Although the exact Cs adsorption site is not determined in the above fitting procedure, since the Cs atoms are at a notable height from the underlying Ag layer ($h_{ad}=3.04$ Å), the Cs atoms are probably located above the Ag atoms and not at the centers of the Ag triangles and Si trimers.

Fig. 3(a) and (b) show the schematics of the Si(111)-$\sqrt{21}\times\sqrt{21}$-(Ag, Cs) and Si(111)-$\sqrt{21}\times\sqrt{21}$-Ag (or Si(111)-$\sqrt{21}\times\sqrt{21}$-(Ag, Au)) surfaces, respectively. In the former surface, Cs adatoms are almost homogeneously distributed while maintaining a triangular lattice with $d_{Cs-Cs}=$ 10.12 Å. In the latter surfaces, Ag or Au adatoms form small triangular islands around the Si trimers with d_{Ag-Ag} or $d_{Au-Au}=6.16$ Å. Why does the above difference appear despite the fact that adatoms are in the monovalent state and have the same $\sqrt{21}\times\sqrt{21}$ periodicity?

Geometrically, the minimum adatom coverage required for $\sqrt{21}\times\sqrt{21}$ periodicity is 1/21 ML. However, experimentally, no $\sqrt{21}\times\sqrt{21}$ periodicities are observed when the coverage is less than 3/21 (=1/7) ML. This implies that when the adatom coverage is less than 3/21 (=1/7) ML, (i) adatoms are not influenced by self-ordering processes and can move freely and/or (ii) the adatoms are mutually and locally bound to form complexes, and such local complexes are randomly distributed.

The Si(111)-$\sqrt{21}\times\sqrt{21}$-Ag (or Si(111)-$\sqrt{21}\times\sqrt{21}$-(Ag, Au)) surface might be explained as the second case mentioned above [25]. When the adatom coverage is low, the Ag or Au adatoms form triangle islands spatially and randomly. With an increase in the adatom coverage, eventually, a $\sqrt{21}\times\sqrt{21}$ periodicity, as shown in Fig. 3(b), is established. Such a change is probably due to the cohesive nature of the Ag and Au atoms. The noble metals have s–d hybridized orbitals and hence the cohesive nature is more prominent in the Ag and Au atoms. On the contrary, the Si(111)-$\sqrt{21}\times\sqrt{21}$-(Ag, Cs) surface might be explained as the first case since the d_{Cs-Cs} value (=10.12 Å) is close to the maximum adatom distance (10.16 Å) when 1/7 ML of adatoms is homogeneously distributed and arranged in a triangular lattice. Probably, Cs atoms are highly mobile when the coverage is low. With an increase in the coverage, each Cs atom is affected by the potentials due to the other atoms and eventually an ordered structure is formed. Even so, because of their weak cohesive nature, Cs atoms do not tend to agglomerate and remain as far as possible from one another. The above difference between noble and alkali metals seems to originate from their electron configurations of the s–d hybridized orbitals or nearly pure s orbitals. Such a scenario might be modeled by considering two-dimensional Friedel oscillations [5].

4. Summary

On the Si(111)-$\sqrt{21}\times\sqrt{21}$-(Ag, Cs) surface, Cs atoms are located at a height of 3.04 ± 0.26 Å from the underlying $\sqrt{3}\times\sqrt{3}$-Ag layer and arrange themselves in a triangular structure with a side length of 10.12 Å in the lateral direction. The structure of the Si(111)-$\sqrt{21}\times\sqrt{21}$-(Ag, Cs) surface is significantly different from that of the Si(111)-$\sqrt{21}\times\sqrt{21}$-Ag and Si(111)-$\sqrt{21}\times\sqrt{21}$-(Ag, Au) surfaces, although $\sqrt{21}\times\sqrt{21}$ periodicity is observed in all cases. This difference is because of the different electronic structures associated with alkali and noble metals.

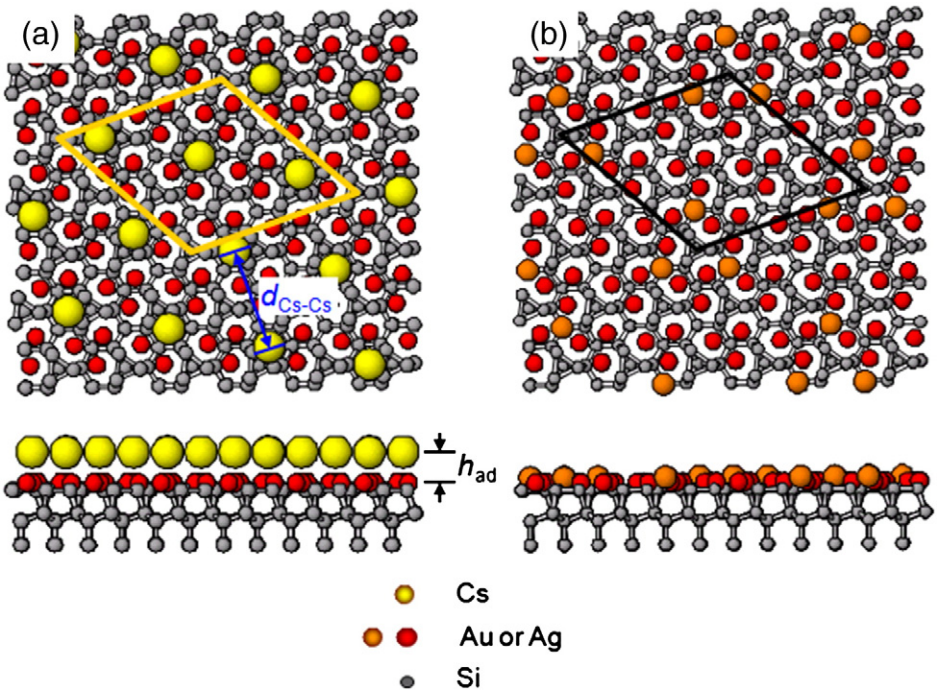

Fig. 3. Schematic of the structures of (a) Si(111)-$\sqrt{21}\times\sqrt{21}$-(Ag, Cs) and (b) Si(111)-$\sqrt{21}\times\sqrt{21}$-Ag and -(Ag, Au) surfaces. Large, medium, and small circles indicate the Cs, Ag (Au), and Si atoms, respectively. A $\sqrt{21}\times\sqrt{21}$ unit cell is denoted by the parallelogram.

Acknowledgment

The present research was partly supported by Grant-in-Aid for Young Scientists (B) 22740205 from JSPS.

References

[1] S. Hasegawa, X. Tong, S. Takeda, N. Sato, T. Nagao, Prog. Surf. Sci. 60 (1999) 89.
[2] S. Hasegawa, J. Phys. Condens. Matter 12 (2000) R463.
[3] T.B. Massalski, U. Mizutani, Prog. Mater. Sci. 22 (1978) 151.
[4] G. Trambly de Laissardière, D. Nguyen-Manh, D. Mayou, Prog. Mater. Sci. 50 (2005) 679.
[5] I. Matsuda, F. Nakamura, K. Kubo, T. Hirahara, S. Yamazaki, W.H. Choi, H.W. Yeom, H. Narita, Y. Fukaya, M. Hashimoto, A. Kawasuso, M. Ono, Y. Hasegawa, S. Hasegawa, K. Kobayashi, Phys. Rev. B 82 (2010) 165330.
[6] Y. Fukaya, I. Matsuda, M. Hashimoto, H. Narita, A. Kawasuso, A. Ichimiya, e-J. Surf. Sci. Nanotechnol. 7 (2009) 432.
[7] J. Nogami, K.J. Wan, X.F. Lin, Surf. Sci. 306 (1994) 81.
[8] A. Ichimiya, H. Nomura, Y. Horio, T. Sato, T. Sueyoshi, M. Iwatsuki, Surf. Rev. Lett. 1 (1994) 1.
[9] X. Tong, Y. Sugiura, T. Nagao, T. Takami, S. Takeda, S. Ino, S. Hasegawa, Surf. Sci. 408 (1998) 146.
[10] H. Tajiri, K. Sumitani, W. Yashiro, S. Nakatani, T. Takahashi, K. Akimoto, H. Sugiyama, X. Zhang, H. Kawata, Surf. Sci. 493 (2001) 214.
[11] C. Liu, I. Matsuda, M. D'angelo, S. Hasegawa, J. Okabayashi, S. Toyoda, M. Oshima, Phys. Rev. B 74 (2006) 235420.
[12] Y. Fukaya, A. Kawasuso, A. Ichimiya, Surf. Sci. 600 (2006) 3141.
[13] Y. Fukaya, A. Kawasuso, A. Ichimiya, Surf. Sci. 601 (2007) 5187.
[14] H. Aizawa, M. Tsukada, Phys. Rev. B 59 (1999) 10923.
[15] H. Jeong, H.W. Yeom, S. Jeong, Phys. Rev. B 76 (2007) 085423.
[16] X. Xie, J.M. Li, W.G. Chen, F. Wang, S.F. Li, Q. Sun, Y. Jia, J. Phys. Condens. Matter 22 (2010) 085001.
[17] H.M. Zhang, K. Sakamoto, R.I.G. Uhrberg, Phys. Rev. B 70 (2004) 245301.
[18] C. Liu, I. Matsuda, H. Morikawa, H. Okino, T. Okuda, T. Kinoshita, S. Hasegawa, Jpn. J. Appl. Phys. 42 (2003) 4659.
[19] A. Kawasuso, T. Ishimoto, M. Maekawa, Y. Fukaya, K. Hayashi, A. Ichimiya, Rev. Sci. Instrum. 75 (2004) 4585.
[20] A. Ichimiya, Surf. Sci. 192 (1987) L893.
[21] A. Ichimiya, Solid State Phenom. 28&29 (1992/93) 143.
[22] A. Ichimiya, Jpn. J. Appl. Phys., Part 1 22 (1983) 176.
[23] G. Radi, Acta Crystallogr. A 26 (1970) 41.
[24] Y. Fukaya, A. Kawasuso, A. Ichimiya, Surf. Sci. 600 (2006) 4086.
[25] N. Sato, T. Nagao, S. Hasegawa, Phys. Rev. B 60 (1999) 16083.